5 g/h of bis(trifluoromethyl) disulfide was delivered to the glow discharge while the metal was vaporized. The desired flow was easily accessible without special metering by allowing the bis(trifluoromethyl) disulfide to slowly vaporize from a chlorobenzene slush (−45 °C). The radio frequency generator power was set at 100 W. After approximately 3 h, the cold finger was allowed to warm and the reaction products were condensed in a −196 °C trap. The products were separated from the unreacted bis(trifluoromethyl) disulfide and plasma gas catenation products by vacuum distillation followed by gas chromatography. The purified product was weighed and a yield, based on the amount of evaporated metal, was calculated.

$Hg(SCF_3)_2$ and $Hg(SCF_3)(CF_3)$. Mercury (1.67 g) was evaporated at a rate sufficient to allow complete evaporation in approximately 3 h. The products were evaporated from the cold finger and vacuum distilled through a −63 °C trap, and the portion retained in the trap was further fractionated by passing through a −15 °C trap. The fraction stopping in the −15 °C trap contained a small amount of the plasma catenation products, 728 mg of $Hg(SCF_3)_2$ (18% yield), 630 mg of $Hg(SCF_3)(CF_3)$ (17% yield), and 51 mg of $Hg(CF_3)_2$ (1.8% yield). The ^{19}F NMR spectra of the $Hg(SCF_3)_2$ product in CH_2Cl_2 gave a singlet at −58 ppm from external CF_3COOH, $J(^{199}Hg-F)$ = 265 Hz, which is in agreement with the values previously reported by Muetterties and co-workers.[4] The second compound, $Hg(SCF_3)(CF_3)$, gave a singlet at −45 ppm from external CF_3COOH for the CF_3 bonded to the mercury, $J(^{199}Hg-F)$ = 1648 Hz. The CF_3 bonded to sulfur gave a singlet at −58 ppm with no observable satellites due to isotope coupling. These findings are consistent with the results reported by Massman and co-workers.[11] The ^{19}F NMR spectrum for $Hg(CF_3)_2$ in methylene chloride gave a singlet at −39.7 ppm from external trifluoroacetic acid with $J(Hg-F)$ = 1295 Hz. The compound appeared identical with $Hg(CF_3)_2$ prepared and purified by other methods.[12,13]

$Te(SCF_3)_2$ and $Te(SCF_3)(CF_3)$. Tellurium (1.34 g) was evaporated over a 3-h period. The products were evaporated from the cold finger and collected in a −196 °C trap. Vacuum distillation of the volatile reaction products through −45, −63, and −95 °C traps resulted in 580 mg of $Te(SCF_3)_2$ (17% yield) being retained in the −45 °C trap while 495 mg of $Te(SCF_3)(CF_3)$ (16% yield) stopped in the −63 °C trap. The unreacted bis(trifluoromethyl) disulfide as well as a yellow impurity passed the −63 °C trap. The ^{19}F NMR spectrum of the impure starting material gave a small singlet at −55.3 ppm from external trifluoroacetic acid with $J(Te-F)$ = 22 Hz. $Te(CF_3)_2$ has a similar color and ^{19}F NMR spectrum and is believed to be the impurity.[12] The concentration of bis(trifluoromethyl)tellurium in the crude CF_3SSCF_3 was estimated to be about 0.30% by gas chromatography. This gives a yield of about 1.5% (40 mg of $Te(CF_3)_2$). $Te(SCF_3)(CF_3)$ was further separated from the plasma catenation products by gas chromatography on a $^3/_8$ in. × 24 ft 10% SE-30 on Chromosorb P column. The $Te(SCF_3)_2$ product was obtained in high purity by condensation on Porapak P contained in a trap on the vacuum line. The contents of this trap were allowed to warm slowly to room temperature, and fractions were collected as they distilled out of the Porapak P. $Te(SCF_3)_2$ was the last fraction to distill off and required overnight pumping and gentle heating (55 °C) to recover all of the material. The product was obtained in greater than 99% purity on the basis of ^{19}F NMR.

$Te(SCF_3)_2$ is a volatile yellow liquid soluble in carbon disulfide.[14] Gas-phase infrared analysis gave bands at 1153 (vs), 1111 (s), 1092 (vs), 752 (m), and 730 (w) cm^{-1}. Mass spectral analysis gave a base peak of *m/e* 69 (CF_3^+ (100%)) and the following comparative abundances of ^{130}Te isotopes (each envelope gave the expected ratio of tellurium and sulfur isotopes): Te^+ (9%), STe^+ (13%), $(SCF_3)Te^+$ (18%), and $(SCF_3)_2Te^+$ (18%). The ^{19}F NMR spectrum gave a singlet at −40.3 ppm from external CF_3COOH with no observable tellurium–fluorine spin–spin coupling.

$Te(SCF_3)(CF_3)$ resembles $Te(SCF_3)_2$ in that it is also a volatile yellow liquid soluble in carbon disulfide. Gas-phase infrared analysis gave bands at 1153 (vs), 1140 (vs), 1098 (s), 1077 (vw), 752 (m), and 728 (m) cm^{-1}. Mass spectral analysis gave a base peak of *m/e* 69 (CF_3^+ (100%)) with the following comparative abundances of Te isotopes: Te^+ (79%), STe^+ (40%), CF_2Te^+ (22%), CF_3Te^+ (81%), $(SCF_3)Te^+$ (74%), and $(CF_3)(SCF_3)Te^+$ (58%). Each of the tellurium-containing fragments occurred in an envelope that had the appropriate distribution of intensities for the isotopes of tellurium and sulfur. The ^{19}F NMR spectrum gave a singlet at −48.5 ppm from external CF_3COOH for the CF_3 bonded to the tellurium, $J(^{125}Te-F)$ = 62 Hz. The CF_3 bonded to sulfur gave a singlet at −38.3 ppm with no observable satellites due to isotope coupling.

Anal. Calcd for $Te(SCF_3)(CF_3)$: S, 10.8; C, 8.1; F, 38.3. Found: S, 11.0; C, 8.3; F, 38.5.

Results and Discussion

The synthesis of (trifluoromethyl)thio organometallic compounds, in spite of the fact that the discharge precursor for this radical is much less specific or selective than in previously reported work, emphasizes one of the strengths of this reaction pathway to σ-bonded organometallic compounds. The advantage is specifically that it is not necessary to have an extremely clean source of radicals in order to affect the reaction. Here the critical factor is simply the statistics of the recombination of metals with radicals. One would expect, and in fact, obtains the statistically expected percentage of the homoleptic compound based on the relative concentrations of each radical present. This is quite in contrast to previous work involving the reaction of radicals with metal halides.[12] This previously reported technique requires extremely clean sources of radicals, for example, the generation of the trifluoromethyl radical from hexafluoroethane, to provide the high yields.

The reaction of (trifluoromethyl)thio radicals generated in a low-temperature glow discharge provides a synthetic route to highly substituted (trifluoromethyl)thio organometallic compounds. In addition to the $\cdot SCF_3$ radical, $\cdot CF_3$ radicals were also produced in a ratio of approximately 2.7 to 1 and resulted in additional products. Reducing the radio frequency power delivered to the plasma had little effect on the ratio of $\cdot SCF_3$ to $\cdot CF_3$ radicals.

Acknowledgment. We are grateful for support of this work by the Air Force Office of Scientific Research, the National Science Foundation, and the Robert A. Welch Foundation.

Registry No. $Hg(SCF_3)_2$, 21259-75-6; $Hg(SCF_3)(CF_3)$, 51353-53-8; $Te(SCF_3)_2$, 83665-28-5; $Te(SCF_3)(CF_3)$, 83665-29-6; Hg, 7439-97-6; Te, 13494-80-9; CF_3SSCF_3, 372-64-5.

---

(11) Flegler, K. H.; Haas, A.; Massmann, H. *Chem. Ztg.* **1973**, *97*, 661.

(12) Lagow, R. J.; Gerchman, L. L.; Jacob, R. A.; Morrison, J. A. *J. Am. Chem. Soc.* **1975**, *97*, 518.

(13) Knunyants, I. L.; Komissarov, Y. F.; Dyatkin, B. L.; Lantseva, L. T. *Izv. Akad. Nauk SSSR, Ser. Khim.* **1973**, *4*, 943.

(14) $Te(SCF_3)_2$ is thermally unstable. After 2 days at ambient temperature, the compound darkens and new peaks can be seen in the ^{19}F NMR. As a result, we could not obtain acceptable analyses. Anal. Calcd for $Te(SCF_3)_2$: S, 19.4; C, 7.3; F, 34.6. Found: S, 17.8; C, 8.4; F, 36.4.

Contribution from the Department of Chemistry,
University of Iowa, Iowa City, Iowa 52242

Carbon-13 NMR Spectroscopy of High-Spin Iron(II) Porphyrin Complexes

Ataollah Shirazi, Eric Leum, and Harold M. Goff*

Received May 13, 1982

A combination of short electronic relaxation times and large zero-field splittings for paramagnetic iron(II) porphyrin species precludes direct ESR measurements but results in sharp, well-resolved NMR spectra. Accordingly, proton NMR studies have previously been used to elucidate the electronic structure, magnetic anisotropy, ligand binding, and aggregation properties of intermediate-spin ($S = 1$) square-planar[1-5] and

---

(1) Goff, H.; LaMar, G. N.; Reed, C. A. *J. Am. Chem. Soc.* **1977**, *99*, 3641.

(2) Mispelter, J.; Momenteau, M.; Lhoste, J.-M. *Mol. Phys.* **1977**, *33*, 1715.

0020-1669/83/1322-0360$01.50/0

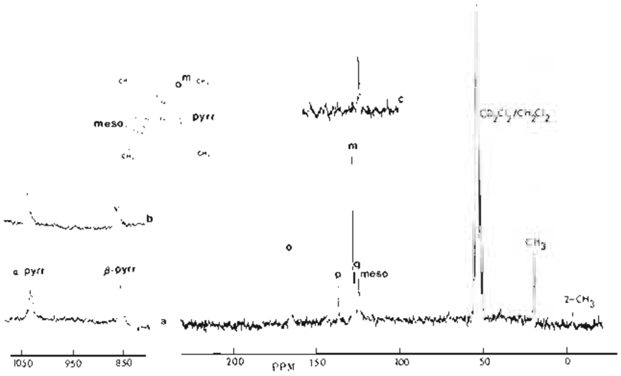

Figure 1. Carbon-13 NMR spectra of high-spin iron(II) porphyrin complexes: (a) Broad-band proton-decoupled spectrum (((p-CH_3)-TPP)Fe 0.03 M, 1,2-dimethylimidazole 0.06 M, CD_2Cl_2/CH_2Cl_2 solvent, 26 °C, $(CH_3)_4Si$ reference, peaks labeled p and q from non-proton-bearing phenyl carbon atoms at the methyl and meso positions, respectively); (b) far-downfield region of the proton-coupled spectrum; (c) signal from (TPP)Fe(1,2-MeIm), which was carbon-13 labeled at the meso-carbon atom.

high-spin ($S = 2$) five-coordinate iron(II) porphyrin species.[6-9] The five-coordinate 2-methylimidazole complexes provide relevant models for deoxyhemoproteins and have been utilized to make proton NMR assignments of far-downfield signals in deoxyhemoglobin and myoglobin.[10] Proton NMR spectra of model high-spin iron(II) porphyrins are characterized by small upfield dipolar shifts and large downfield contact shifts for pyrrole substituents.[6,7] The meso proton curiously experiences a small upfield contact shift. Carbon-13 spectral work described here was undertaken in an effort to better understand delocalization of unpaired spin density for paramagnetic metalloporphyrins in general and for high-spin iron(II) porphyrins in particular.

Experimental Section

Isolated bis(piperidine) complexes of iron(II) tetratolylporphyrins, [$((CH_3)TPP)Fe(pip)_2$], were prepared by piperidine reduction of the iron(III) chloride complex.[11,12] The bis(pyridine) complexes of iron(II) octaethylporphyrin, [$(OEP)Fe(py)_2$], and etioporphyrin I, [$(ETIO)Fe(py)_2$], were prepared and handled under a nitrogen atmosphere with use of hydrazine hydrate as a reducing agent.[13] Solid samples were placed in a 10-mm NMR tube with an attached ground-glass joint and a restricted top for sealing. The NMR tube was attached to a vacuum line and heated to 150–160 °C in an oil bath for either 2 h (OEP and ETIO complexes) or 12 h (TPP complexes). This operation served to remove the axial ligands, leaving the square-planar species. In a separate tube on the vacuum line the appropriate volume of purified solvent containing 1,2-dimethylimidazole was degassed through freeze–pump–thaw cycles. This mixture was then distilled into the NMR tube, and the tube was sealed by torch. Proton NMR spectra were recorded to confirm identity of the five-coordinate complexes. Both proton and carbon-13 spectra were recorded on a JEOL FX-90Q FT NMR spectrometer.

Table I. Carbon-13 NMR Spectra of (1,2-Dimethylimidazole)iron(II) Porphyrin Complexes

	iron(II) porphyrin			
C atom	((p-CH_3)-TPP)Fe[a]	((m-CH_3)-TPP)Fe[b]	(OEP)Fe[d]	(ETIO)Fe[d]
α-pyrr	1032 (200)	1019	990[e]	1024
β-pyrr	850 (150)	834	763[e]	788
meso	125.6	125.0	94.2	97.7
quat Ph	127.7	~128.		
ortho Ph	166.8	167.3, 163.1		
meta Ph	128.6	137.6, 128.6		
para Ph	137.8	128.6		
CH_3–Ph	20.0	22.7		
ring CH_2			100.3	105.0
ring CH_3				101.5
ethyl CH_3			44.8	43.1
Im 2-C		~890[c]		
Im 4-C		~390[c]		
Im 5-C		~96[c]		
Im 1-CH_3		~106[c]		
Im 2-CH_3		~−20[c]		

[a] Conditions: Iron porphyrin 0.03 M; 1,2-dimethylimidazole 0.06 M; 26 °C; CD_2Cl_2/CH_2Cl_2 solvent; referenced to $(CH_3)_4Si$. Downfield shifts in ppm are given a positive sign. Values in parentheses are line widths in hertz. [b] Conditions: Iron porphyrin 0.04 M; 1,2-dimethylimidazole 0.06 M; 26 °C; CH_2Cl_2 solvent. [c] Extrapolated value for coordinated ligand at 27 °C based on solutions 0.01 M in ((m-CH_3)TPP)Fe and either 0.10 or 0.25 M in 1,2-dimethylimidazole. [d] Conditions: Saturated in iron porphyrin, ~0.01 M; 1,2-dimethylimidazole 0.04 M; 26 °C; C_6H_6 solvent. [e] CH_2Cl_2 solvent.

Results and Discussion

Addition of sterically hindered imidazoles to iron(II) porphyrins provides a ready means of generating the five-coordinate high-spin state. For 2-methylimidazole in benzene solution at 34 °C, equilibrium constants are 2×10^3 and 2×10^4 M^{-1} for (OEP)Fe and (TPP)Fe, respectively.[7] Ease of vacuum line transfer and enhanced solubility of the five-coordinate product directed use of 1,2-dimethylimidazole for this work. With the assumption of comparable equilibrium constants for 1,2-dimethylimidazole, the inclusion of 0.02 M excess 1,2-dimethylimidazole at 26 °C is expected to convert >99% of (TPP)Fe and >98% of (OEP)Fe to the five-coordinate complexes. This was further confirmed through examination of the proton NMR spectra.[6,7]

The proton-decoupled carbon-13 spectrum of ((p-CH_3)-TPP)Fe(1,2-MeIm) is shown in Figure 1a. Signals in a far-downfield position logically belong to pyrrole carbon atoms on the basis of assignments for high-spin iron(III) porphyrin complexes.[14-19] The signal at 850 ppm is split into a doublet in the proton-coupled spectrum as indicated in Figure 1b, whereas the 1032-ppm signal represents a non-proton-bearing carbon atom. Assignments for pyrrole α- and β-carbon signals are thus readily made. The meso-carbon signal is directly assigned through examination of meso-carbon-13 enriched (TPP)Fe(1,2-MeIm). As shown in Figure 1c, the signal is located at 124.4 ppm. Assignment of phenyl signals was possible through examination of m- and p-methyl TPP complexes in combination with proton-coupled and proton-decoupled experiments. Chemical shift values for meta- and

---

(3) Wayland, B. B; Mehne, L. F.; Swartz, J. *J. Am. Chem. Soc.* **1978**, *100*, 2379.

(4) Mispelter, J.; Momenteau, M.; Lhoste, J.-M. *J. Chem. Phys.* **1980**, *72*, 1003.

(5) Migita, K.; LaMar, G. N. *J. Phys. Chem.* **1980**, *84*, 2953.

(6) Goff, H.; LaMar, G. N. *J. Am. Chem. Soc.* **1977**, *99*, 6599.

(7) Mispelter, J.; Momenteau, M.; Lhoste, J.-M. *Chem. Phys. Lett.* **1978**, *57*, 405.

(8) Parmely, R. C.; Goff, H. M. *J. Inorg. Biochem.* **1980**, *12*, 269.

(9) Mispelter, J.; Momenteau, M.; Lhoste; J.-M. *Biochimie* **1981**, *63*, 911.

(10) LaMar, G. N.; Budd, D. L.; Goff, H. *Biochem. Biophys. Res. Commun.* **1977**, *77*, 104.

(11) Epstein, L. M.; Straub, D. K.; Maricondi, C. *Inorg. Chem.* **1967**, *6*, 1720.

(12) Radonovich, L. J.; Bloom, A.; Hoard, J. L. *J. Am. Chem. Soc.* **1972**, *94*, 2073.

(13) Dolphin, D.; Sams, J. R.; Tsin, T. B.; Wong, K. L. *J. Am. Chem. Soc.* **1976**, *98*, 6970.

(14) Goff, H. *Biochim. Biophys. Acta* **1978**, *542*, 348.

(15) Mispelter, J.; Momenteau, M.; Lhoste, J.-M. *J. Chem. Soc., Chem. Commun.* **1979**, 808.

(16) Phillippi, M. A.; Goff, H. M. *J. Chem. Soc., Chem. Commun.* **1980**, 455.

(17) Mispelter, J.; Momenteau, M.; Lhoste, J.-M. *J. Chem. Soc., Dalton Trans.* **1981**, 1729.

(18) Phillippi, M. A.; Baenziger, N.; Goff, H. M. *Inorg. Chem.* **1981**, *20*, 3904.

(19) Goff, H. M.; Shimomura, E. T.; Phillippi, M. A. *Inorg. Chem.*, in press.

para-carbon atoms and attached methyl groups listed in Table I are very close to those of diamagnetic metalloporphyrins.[20] The signal at 166.8 ppm is that of a proton-bearing carbon atom, and the signal is split (167.3 and 163.1 ppm) for the *m*-tolyl analogue, thus indicating the ortho-carbon assignment. A non-proton-bearing carbon signal at 127.7 ppm is assigned to the remaining quaternary phenyl carbon atom. Although porphyrin carbon-13 signals follow general Curie-law behavior, poor solubility of the five-coordinate complexes at low temperature precluded a complete temperature dependence study.

Spectra for (OEP)Fe and (ETIO)Fe complexes were recorded in both CH_2Cl_2 and C_6H_6 solvents at temperatures from 16 to 55 °C. (Slow oxidation of the iron(II) species was noted for the chlorinated solvent.) Spectral assignments are listed in Table I. Pyrrole carbon assignments are based on the ordering observed for the (TPP)Fe species. Further analogy to the (TPP)Fe complexes suggested that the meso-carbon signal of (OEP)Fe(1,2-MeIm) and (ETIO)Fe(1,2-MeIm) would be near the diamagnetic value (~97 ppm). This is indeed the case, as the 94.2-ppm signal for the (OEP)Fe complex was resolved as a doublet in the proton-coupled spectrum. Proton coupling patterns for the 100.3- and 44.8-ppm signals also permitted respective assignments to the CH_2 and CH_3 groups.

Although the solutions prepared for carbon-13 spectral studies contained excess 1,2-dimethylimidazole, no resonances corresponding to free ligand positions were noted. Small, sharp signals such as the one at −3.4 ppm in Figure 1a were detected, however. The positions of these signals were strongly dependent on the relative amounts of free and coordinated ligand. Thus, rapid ligand exchange on the carbon-13 NMR time scale was suggested, much as was previously discerned for proton NMR measurements.[6,7] Poor solubility precluded "freezing out" ligand exchange at low temperatures. accordingly, the coordinated ligand chemical shift values were estimated from experiments where 1,2-dimethylimidazole was added in excess, and it was assumed that the observed ligand chemical shifts were mole fraction weighted with respect to concentrations of free and coordinated ligand. Solutions were examined that contained 0.01 M ((m-CH_3)TPP)Fe and either 0.10 or 0.25 M 1,2-dimethylimidazole. Reasonable agreement between calculated values for these two solutions supports the assumption of dynamics at the near-fast-exchange limit. Estimated chemical shift values for coordinated 1,2-dimethylimidazole are listed in Table I.

Large downfield pyrrole carbon shifts are expected for the high-spin d^6 configuration as a consequence of strong interaction between the σ-type $d_{x^2-y^2}$ unpaired spin and pyrrole nitrogen atoms. Likewise, large downfield shifts for imidazole 2- and 4-carbon atoms are likely due to unpaired spin in the d_{z^2} orbital. Effects of π-type spin delocalization from unpaired spin in the d_{xz}, d_{yz} set are less evident for the high-spin iron(II) porphyrins than for corresponding five-coordinate high-spin iron(III) complexes. Thus, the iron(III) derivatives exhibit pyrrole carbon signals in the 1200–1300-ppm region.[16-19] The pyrrole β-carbon signal is broader than the pyrrole α-carbon signal of high-spin iron(III) porphyrins. This is likely a consequence of large π unpaired spin density delocalized through the $3e(\pi)$ molecular orbital[17] (which has larger amplitude at the pyrrole β-carbon atom[21]). Reversal of pyrrole carbon line widths and smaller isotropic shift values for high-spin iron(II) complexes are indicative of smaller π spin density contributions. The pyrrole ethyl carbon atoms of (OEP)Fe species also reflect the degree of π spin delocalization, which should give the CH_2 resonance an upfield bias and the CH_3 resonance a downfield shift. This effect is apparent in CH_2 and CH_3 signals of 100.3 and 44.8 ppm for (OEP)-Fe(1,2-MeIm) vs. respective values of 75.0 and 149.0 ppm for (OEP)FeCl.[14]

The meso-carbon signal of ((p-CH_3)TPP)Fe(1,2-MeIm) exhibits a downfield shift (isotropic shift) of only 5.7 ppm when compared with that for a diamagnetic cobalt(III) analogue.[20] In terms of the spin delocalization pattern, this small meso-carbon shift is deceptive. Thus, isotropic shifts for the attached phenyl carbon, the ortho carbon, and the meso proton (of the (OEP)Fe complex) are −9.6, +33, and −9 ppm, respectively. The pattern of alternating shift direction is reminiscent of that for five-coordinate high-spin iron(III) complexes,[16-19] although shifts are approximately an order of magnitude greater for the higher oxidation state species. This shift pattern may be described by a polarization mechanism in which positive π spin density at the meso-carbon atom induces σ-type spin density in attached phenyl groups. The relatively small π spin density at the meso-carbon atom reasonably reflects a minor contribution of spin delocalization through the $4e(\pi^*)$ MO (which exhibits large amplitude at the meso-carbon position[21]). Controversy over interpretation of previous proton NMR results has centered on the degree of π spin delocalization in high-spin iron(II) porphyrins.[6,7] Carbon-13 spectroscopy provides a better view of the entire macrocycle, and it may safely be stated that π spin density in high-spin iron(II) porphyrins is a fraction of that in iron(III) analogues. Attenuation of pyrrole carbon shifts also implies diminished σ spin delocalization in iron(II) vs. iron(III) porphyrins. The apparent importance of electrostatic interactions will be investigated by carbon-13 methods for other metalloporphyrin species.

In more empirical terms, the model study presented here provides a basis for carbon-13 NMR examination of deoxyhemoproteins and also strategy for carbon-13 label incorporation into the macromolecules. Porphyrin ring methyl and methylene as well as meso-carbon and imidazole 5-carbon signals should be found in the 90–100-ppm region, reasonably isolated from the bulk of protein signals. Unfortunately, the potential overlap of these several paramagnetic signals will complicate assignments. Signals far downfield of the diamagnetic region are expected for pyrrole carbon atoms and for the imidazole 2-carbon and 4-carbon signals. Severe line broadening will likely preclude observation of these resonances in the absence of label incorporation.

Acknowledgment. Support from NIH Grant GM28831-02 is gratefully acknowledged.

Registry No. ((p-CH_3)TPP)Fe(1,2-MeIm), 83547-71-1; ((m-CH_3)TPP)Fe(1,2-MeIm), 83547-72-2; (OEP)Fe(1,2-MeIm), 75811-16-4; (ETIO)Fe(1,2-MeIm), 83547-73-3.

---

[20] Goff, H. M. *J. Am. Chem. Soc.* **1981**, *103*, 3714.

[21] LaMar, G. N.; Walker, F. A. In "The Porphyrins"; Dolphin, D., Ed.; Academic Press: New York, 1979; Vol. IV, pp 61-157.

Contribution from the Département de Recherches Physiques
(LA 71), Université Pierre et Marie Curie,
75230 Paris Cedex 05, France,
Laboratoire de Chimie (LA 32), Ecole Normale Supérieure,
75231 Paris Cedex 05, France, and Institut de Chimie (LA 31),
Université Louis Pasteur, 67008 Strasbourg, France

Resonance Raman Spectra of Metalloporphyrins with a Ligand Inserted between the Metal and a Pyrrole Nitrogen

G. Chottard,*[1a] D. Mansuy,[1b] and H. J. Callot[1c]

Received May 18, 1982

Resonance Raman (RR) spectroscopy has been successfully used in recent years to gain insight into the structure of he-